Journal of
MATERIALS RESEARCH

Sensitizing effect of Yb^{3+} on near-infrared fluorescence emission of Cr^{4+}-doped calcium aluminate glasses

Yong Gyu Choi[a] and Kyong Hon Kim
Telecommunication Basic Research Laboratory, Electronics and Telecommunications Research Institute (ETRI), Yusong P.O. Box 106, Taejon 305-600, Korea

Yong Seop Han and Jong Heo
Photonic Glasses Laboratory, Department of Materials Science and Engineering, Pohang University of Science and Technology (POSTECH), San 31, Hyoja-dong, Nam-gu, Pohang, Kyungbuk 790-784, Korea

(Received 6 June 1999; accepted 4 November 1999)

We have demonstrated that an efficient energy transfer takes place from Yb^{3+} to Cr^{4+} in calcium aluminate glasses. Yb^{3+} improves excitation efficiency at around 980 nm, enhancing emission intensity of Cr^{4+} fluorescence at 1.2–1.6 μm. Nonradiative energy transfer via electric dipole–dipole interaction between ytterbium and chromium ions was found to be dominant over radiative $Yb^{3+} \rightarrow Cr^{4+}$ energy transfer. A diffusion-limited energy transfer mechanism well explains the decay behavior of Yb^{3+}/Cr^{4+}-codoped glasses. This codoping scheme may be applicable to other Cr^{4+}-containing crystals and glasses.

Conventional oxide glasses exhibit strong adsorption in the 3.5–5 μm region, while infrared (IR) transmission cutoff of calcium aluminate glasses is around 6 μm wavelength, which is mainly attributed to low vibrational energy (~700 cm^{-1}) of these glasses compared to that (typically higher than 900 cm^{-1}) of the conventional oxide glasses.[1] Calcium aluminate glasses have been estimated to show the sum of scattering losses of approximately 0.04 dB/km at 1.55 μm.[2] In addition, these glasses exhibit a mechanical strength comparable to that of some silicate glasses.[3] On the other hand, binary CaO–Al_2O_3 glasses have a narrow glass-forming region and a pronounced tendency toward devitrification. However, introduction of alkali and alkaline-earth metals to the calcium aluminate system significantly improves the glass-forming ability.[4] On the basis of the above considerations, calcium aluminate glasses can be applicable to telecommunication uses. Renewed interests on these glasses have risen since stable formation of the +4 oxidation state of chromium dopant, which emits near-infrared luminescence, has been known.[5]

Cr^{4+} ion under specific fourfold crystal fields in some oxide glasses emits 1.2–1.6 μm fluorescence which is attributed to an intra-$3d^2$ configurational transition. So far, formation of the stable +4 oxidation state of chromium has been achieved only in calcium-aluminate and alumino-silicate glasses.[6,7] There is still lack of understanding associated with the processing condition and mechanism of Cr^{4+} formation in glasses. For example, incorporation of Cr^{4+} into fourfold coordination sites was promoted when these glasses were melted under an inert atmosphere.[6] However, the content of Cr^{4+} ions was independent of melting atmosphere, and the relative content of Cr^{6+} increased with increasing oxygen partial pressure of the melting atmosphere.[7]

In T_d symmetry, the Cr^{4+}: $^3A_2 \rightarrow {}^3T_1$ absorption transition is electric dipole allowed while the $^3A_2 \rightarrow {}^3T_2$ transition is electric dipole forbidden.[7] However, due to the asymmetric phonons originated from distortion of the perfect tetrahedron, the $^3A_2 \rightarrow {}^3T_2$ transition can become partially allowed. Therefore, strong absorption bands in the visible region are attributed to the $^3A_2 \rightarrow {}^3T_1$ transition, while the weak near-infrared absorption is most likely arising from the $^3T_2$ level (Fig. 1). On the other hand, an excited-state absorption (ESA) conspicuously occurs at the visible wavelength in Cr^{4+}-doped crystals.[9,10] The same phenomenon is also evident in Cr^{4+}-doped calcium aluminate glasses.[6] This means that optical pumping with wavelength longer than ~900 nm, where the absorption efficiency is low, is better to avoid the ESA. However, a significant ground-state absorption between 1200 and 1500 nm takes place even in a glass doped with low concentration of Cr, i.e., 0.1 mol% Cr_2O_3 [Fig. 1(a)], which reabsorbs the Cr^{4+}:$^3T_2 \rightarrow {}^3A_2$ luminescence responsible for the 1.2–1.6 μm fluorescence and thereby makes a deleterious effect by lowering the corresponding quantum efficiency. Increase of doping concentration of the chromium ions to enhance the ab-

[a]Address all correspondence to this author.

sorption at the $^3T_2$ level is also prohibited due to the probable concentration quenching effect.[8] Thus, Cr concentration should be kept low and an efficient pump mechanism is required for the chromium-doped crystals and glasses for laser and amplifier applications.

In this paper, Yb^{3+} ion, of which the strong absorption peak is around 980 nm, is introduced as a sensitizer of Cr^{4+} ion in calcium–aluminate glasses in order to provide a suitable pump band. Spectral overlap between Yb^{3+} emission and Cr^{4+} absorption and the relatively high oscillator strength of Cr^{4+} provide the theoretically adequate backgrounds of $Yb^{3+} \rightarrow Cr^{4+}$ energy transfer.

$51CaO–36Al_2O_3–10BaO–3ZnO$ (mol%) glasses doped with Cr_2O_3 and (or) Yb_2O_3 were prepared in air by the conventional melt-quenching method. Starting materials with purity higher than 99.9% were weighed and mixed to yield 10-g-batch mixtures. The glass samples were obtained by melting the mixtures in Pt crucibles at 1650 °C for 1 h and subsequent annealing at 700 °C. Up to 1.0 mol% Yb_2O_3 could be dissolved in our host composition without any sign of crystallization. A charge-transfer band of Cr^{6+} as well as the intraconfigurational transitions of Cr^{4+} are resolved in the low-intensity absorption spectrum of the Cr_2O_3-doped glasses [Fig. 1(a)]. Absorption from Yb^{3+} [Fig. 1(c)] is well overlapped with the absorption of the Cr^{4+}: $^3A_2 \rightarrow {}^3T_2$ transition [Fig. 1(b)]. Using a 978-nm pump, fluorescence emission enhanced in magnitude at room temperature is evident in a glass codoped with 0.01 mol% Cr_2O_3 and 1.0 mol% Yb_2O_3 (Fig. 2). The full width at half-maximum of the fluorescence in the 1.2–1.6-μm band is about 190 nm. Figure 3 shows the fluorescence decay profiles of Yb^{3+}:$^2F_{5/2} \rightarrow {}^2F_{7/2}$ transition. An exponential decay with the 1/e fall time of 822 μs is evident in the 1.0 mol% Yb_2O_3 single-doped glass [Fig. 3(a)]. This measured lifetime is comparable with a radiative transition prob-

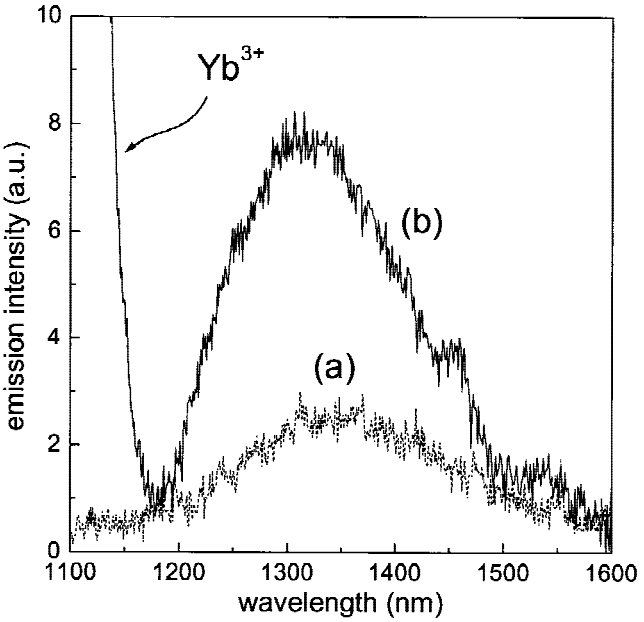

FIG. 2. Fluorescence emission spectra of calcium aluminate glasses doped with (a) 0.01 mol% Cr_2O_3 only and (b) 0.01 mol% Cr_2O_3/1.0 mol% Yb_2O_3. Excitation wavelength was at 978 nm, the peak wavelength of the Yb^{3+} absorption spectrum.

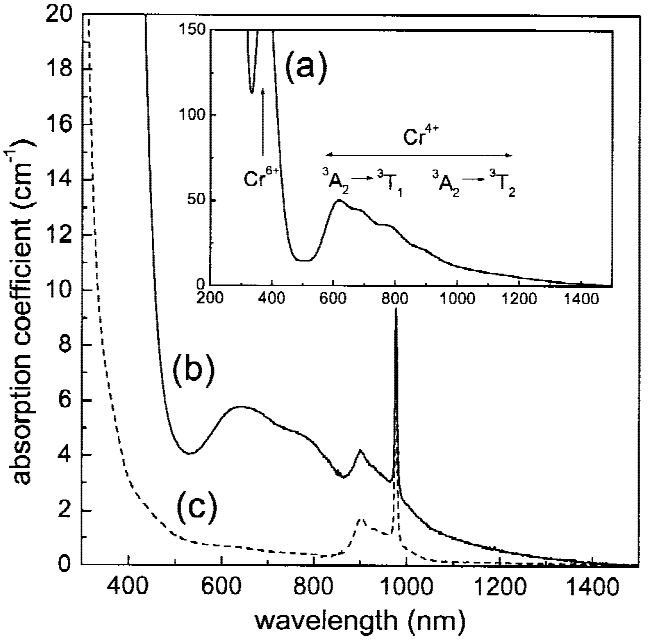

FIG. 1. Low-intensity absorption spectra of calcium aluminate glasses doped with (a) 0.1 mol% Cr_2O_3, (b) 0.01 mol% Cr_2O_3/1.0 mol% Yb_2O_3, and (c) 1.0 mol% Yb_2O_3, respectively.

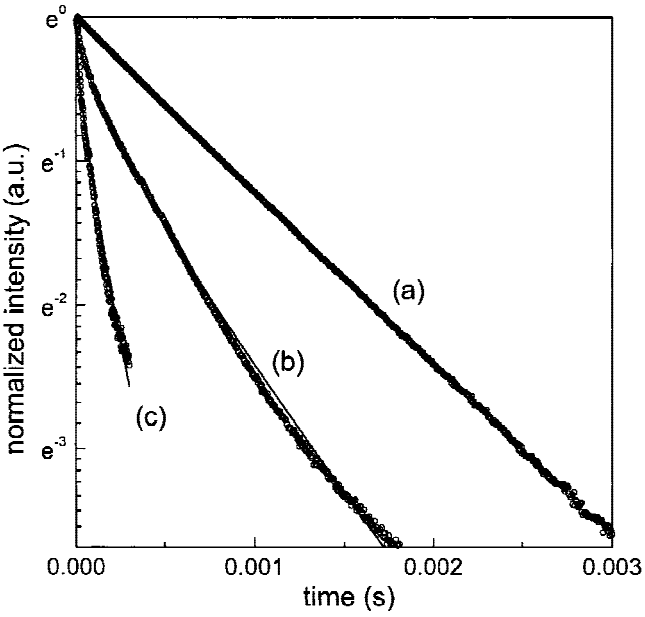

FIG. 3. Fluorescence decay curves of the Yb^{3+}: $^2F_{5/2} \rightarrow {}^2F_{7/2}$ transition for 1.0 mol% Yb_2O_3-doped glasses with Cr_2O_3 doping concentrations of (a) 0, (b) 0.01, and (c) 0.1 mol%, respectively. Solid lines were obtained from the least-squares fit to Eq. (2).

ability of Yb^{3+} in this glass host (~1049 ± 10 s^{-1}), which is calculated from the absorption spectrum using the Fuchtbauer–Ladenburg equation.[11] This indicates that the radiative transition rate of Yb^{3+} is hardly affected by the phonon environment. Meanwhile, when the concentration of Cr_2O_3 is increased from 0.01 to 0.1 mol%, the decay profiles result in shortened decay times and clear nonexponential decay behaviors [Figs. 3(b) and 3(c)]. Such a nonexponential decay suggests that there is an energy transfer from ytterbium ion to another ion, most probably chromium ion in this case.

When the activators or quenching centers are present, a decaying behavior of the sensitizer fluorescence follows a nonexponential behavior at the beginning. At the later stage of the decay, however, an exponential behavior starts to dominate because of either the energy migration among sensitizer ions or ceasing of donor–acceptor energy transfer.[12] In general, both direct sensitizer → activator energy transfer and diffusion among sensitizer ions affect overall decay behavior of a sensitizer. An overall deexcitation probability $N(t)$ with time t is expressed as follows:

$$N(t) = \exp\{-W_0 t - \Pi(t)\} \quad , \tag{1}$$

where W_0 is a reciprocal of lifetime without any energy acceptor and $\Pi(t)$ is a magnitude of the departure from the intrinsic exponential behavior due to the energy transfer between sensitizer and activator ions. In a multipole–multipole interaction scheme, $\Pi(t)$ is proportional to $t^{3/s}$, where the exponent s can be either 6, 8, or 10 depending upon the electric-multipole character of the sensitizer–activator interaction.[13] Then, the exponent of $\Pi(t)$ can be revealed from a slope in the plot of $\ln\{-\ln N(t) - W_0 t\}$ versus $\ln(t)$. It is verified in Fig. 4 that the slope is 0.74 and 0.62 for 0.01 and 0.1 mol% Cr_2O_3 doped glasses, respectively. The slightly higher value than 0.5 for the exponent of $\Pi(t)$, i.e., $s = 6$, may suggest that a considerable amount of diffusion among Yb^{3+} ions intervenes in the time scale of our observation. The decrease in the exponent with increasing chromium concentration further indicates that the effect of direct energy transfer becomes dominant as the chromium concentration increases. Therefore, both diffusion among sensitizer ions and single step electric dipole–dipole transfer from sensitizers to randomly distributed activator ions should be considered, and the following equation derived by Yokota and Tanimoto[14] was used for the fits of experimental decay curves:

$$N(t) = \exp\left\{ - W_0 t - \tfrac{4}{3}\pi^{3/2} n_a C_{sa}^{1/2} t^{1/2} \left(\frac{1 + 10.87x + 15.50x^2}{1 + 8.743x} \right)^{3/4} \right\} \quad . \tag{2}$$

Here, n_a is an activator concentration, C_{sa} is an interaction parameter, and $x = DC_{sa}^{-1/3} t^{2/3}$, where D is a diffusion coefficient for energy migration among donors. Then, the critical transfer distance R_0 can be calculated from an equation, $R_0^6 = C_{sa}/W_0$. For an isolated sensitizer–activator pair separated by R_0, the energy transfer occurs with the same rate as the spontaneous deactivation in the sensitizer. The optimized R_0 was estimated to be 4 ± 1 nm using results of the least-squares fits in Figs. 3(b) and 3(c). The distance is larger than that of $Eu^{3+} \rightarrow Cr^{3+}$ transfer in a phosphate glass.[15]

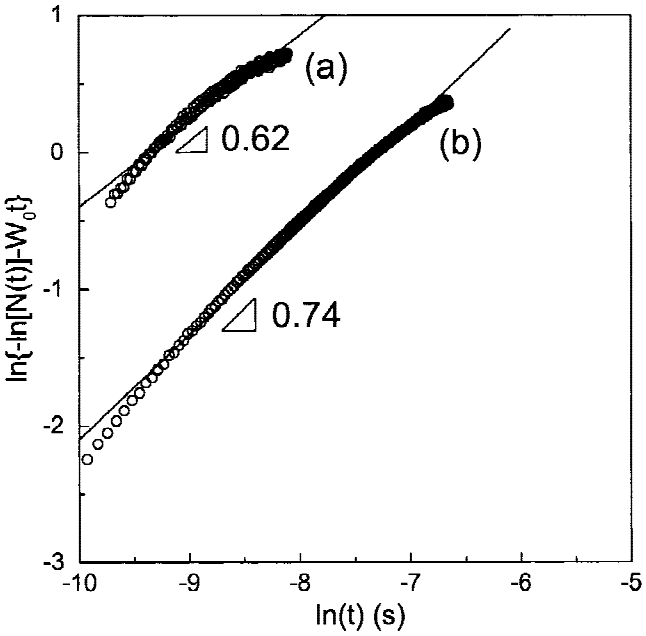

FIG. 4. Dependence of $\Pi(t)$ on $\ln(t)$ for 1.0 mol% Yb_2O_3-doped glasses with codopant of (a) 0.1 and (b) 0.01 mol% Cr_2O_3, respectively. Solid lines were plotted from the least-squares fit to the straight line.

Radiative energy transfer was also appreciable in the Yb^{3+}/Cr^{4+}-codoped glasses, since the spectral shape of the Yb^{3+}: $^2F_{5/2} \rightarrow {}^2F_{7/2}$ transition was distorted according to the absorption line shape of Cr^{4+} around Yb^{3+} emission wavelength. On the other hand, a back energy transfer from chromium to ytterbium seems not to be plausible. The measured lifetimes of the infrared emission in calcium aluminate glasses are in a range of submicroseconds to ~40 μs at room temperature, and the fast transition rates mainly result from the strong nonradiative multiphonon relaxation.[5,16]

In conclusion, we have demonstrated improvement of 980-nm pump efficiency as well as enhancement of 1.2–1.6 μm fluorescence of Cr^{4+}-doped calcium aluminate glasses by introduction of Yb^{3+} as a sensitizer. Electric dipole–dipole energy transfer from Yb^{3+} to Cr^{4+}, which is limited by diffusion among Yb^{3+} ions, is a dominant energy transfer mechanism. This codoping scheme may be applicable to other Cr^{4+}-containing crystals and glasses.

ACKNOWLEDGMENTS

Work at ETRI was supported by the Ministry of Information and Communication of Korea. Work at POSTECH was supported in part by the Korean Science and Engineering Foundation (KOSEF) through the Ultra-Fast Fiber-Optic Networks Research Center at Kwangju Institute of Science and Technology.

REFERENCES

1. Y.G. Choi and J. Heo, J. Non-Cryst. Solids **217,** 199 (1997).
2. M.E. Lines, J.B. MacChesney, K.B. Lyons, A.J. Bruce, A.E. Miller, and K. Nassau, J. Non-Cryst. Solids **107,** 251 (1989).
3. G.Y. Onoda, Jr., and S.D. Brown, J. Am. Ceram. Soc. **53,** 311 (1970).
4. E.V. Uhlmann, M.C. Weinberg, N.J. Kreidl, and A.A. Goktas, J. Am. Ceram. Soc. **76,** 449 (1994).
5. K. Cerqua-Richardson, B. Peng, and T. Izumitani, OSA Proc. Adv. Solid-State Lasers **13,** 52 (1992).
6. E. Munin, A.B. Villaverde, M. Bass, and K. Cerqua-Richardson, J. Phys. Chem. Solids **58,** 51 (1997).
7. T. Murata, M. Torisaka, H. Takebe, and K. Morinaga, J. Non-Cryst. Solids **220,** 139 (1997).
8. M.J. Weber, J. Appl. Phys. **44,** 4058 (1973).
9. Z. Burshtein, P. Blau, Y. Kalisky, Y. Shimony, and M.R. Kokta, IEEE J. Quantum Electron. **34,** 292 (1998).
10. V.P. Mikhailov, N.I. Zhavoronkov, N.V. Kuleshov, A.S. Avtukh, and V.G. Shcherbitsky, Opt. Quantum Electron. **27,** 767 (1995).
11. H. Takebe, T. Murata, and K. Morinaga, J. Am. Ceram. Soc. **79,** 681 (1996).
12. I.A. Bondar, A.I. Burshtein, A.V. Krutikov, L.P. Mezentseva, V.V. Osiko, V.P. Sakun, V.A. Smirnov, and I.A. Shcherbakov, Sov. Phys. JETP **54,** 45 (1981).
13. D.L. Dexter, J. Chem. Phys. **21,** 836 (1953).
14. M. Yokota and O. Tanimoto, J. Phys. Soc. Jpn. **22,** 779 (1967).
15. M.J. Weber, Phys. Rev. **B4,** 2932 (1971).
16. X. Wu, H. Yuan, W.M. Yen, and B.G. Aitken, J. Lumin. **66&67,** 285 (1996).